

Temporal quantum control with graphene

This article has been downloaded from IOPscience. Please scroll down to see the full text article.

2012 New J. Phys. 14 123020

(<http://iopscience.iop.org/1367-2630/14/12/123020>)

View [the table of contents for this issue](#), or go to the [journal homepage](#) for more

Download details:

IP Address: 84.78.211.145

The article was downloaded on 13/12/2012 at 11:14

Please note that [terms and conditions apply](#).

Temporal quantum control with graphene

A Manjavacas^{1,3}, S Thongrattanasiri¹, D E Chang²
and F J García de Abajo^{1,3}

¹ IQFR—CSIC, Serrano 119, E-28006 Madrid, Spain

² ICFO-Institut de Ciències Fòniques, Mediterranean Technology Park,
E-08860 Castelldefels, Barcelona, Spain

E-mail: a.manjavacas@csic.es and J.G.deAbajo@csic.es

New Journal of Physics **14** (2012) 123020 (12pp)

Received 20 August 2012

Published 12 December 2012

Online at <http://www.njp.org/>

doi:10.1088/1367-2630/14/12/123020

Abstract. We introduce a novel strategy for controlling the temporal evolution of a quantum system at the nanoscale. Our method relies on the use of graphene plasmons, which can be electrically tuned in frequency by external gates. Quantum emitters (e.g. quantum dots) placed in the vicinity of a graphene nanostructure are subject to a strong interaction with the plasmons of this material, thus undergoing time variations in their mutual interaction and quantum evolution that are dictated by the externally applied gating voltages. This scheme opens a new path towards the realization of quantum-optics devices in the robust solid-state environment of graphene.

Control of the temporal quantum evolution of a physical system by means of external macroscopic stimuli will make versatile quantum-information devices viable [1]. Various methods for quantum control have been proposed [1], and despite efforts and progress in fields such as ion traps [2, 3], scalable systems remain an open challenge. In recent years solid-state quantum devices have attracted growing interest, because they provide a robust platform for implementing scalable temporal control [4, 5]. In this paper, we show that doped graphene nanostructures combined with two-level atoms or quantum dots provide a robust platform for achieving the desired goal of full temporal quantum control. The interaction

³ Authors to whom any correspondence should be addressed.



Content from this work may be used under the terms of the [Creative Commons Attribution-NonCommercial-ShareAlike 3.0 licence](https://creativecommons.org/licenses/by-nc-sa/3.0/). Any further distribution of this work must maintain attribution to the author(s) and the title of the work, journal citation and DOI.

between the quantum dots is strongly mediated by plasmons in the graphene, which can be electrostatically tuned through engineered gates [6, 7]. The quantum evolution of the dots is then manipulated by modulating the electric potential we apply to the gates over time. We provide realistic simulations demonstrating excellent control over the decay of individual and interacting dots. Any desired decay profile can be produced by resorting to the unprecedentedly fast electro-optical modulation of graphene [8] and its strong interaction with neighboring quantum emitters [9]. This constitutes a radically new path toward controlling quantum systems in nanoscale solid-state environments by means of conventional electronics, with the capacity for bringing quantum devices closer to reality.

Quantum mechanics rules the temporal evolution at small length and energy scales, giving rise to non-intuitive properties such as quantum superposition and entanglement. These phenomena provide an extra handle to process information [10, 11], to improve optical metrology and break the imaging diffraction limit [12], and to substantially alter the statistics of light [13–15], with a vast range of potential applications, including quantum computing and cryptography [16] and sensing [12]. However, controlling the quantum evolution at such length and energy scales remains a challenge that can only be partially addressed by using elaborate setups, for example in the context of cavity quantum electrodynamics [1, 3, 17]. Recently, surface plasmons have been identified as a potential candidate to mediate the interaction between externally controlled signals (e.g. laser beams) and small quantum systems (e.g. quantum dots), allowing one to explore exciting phenomena such as single photon transistors [18], entanglement [19] and quantum blockade [20], among other feats. In the following, we show that graphene can also be used to control the evolution of a quantum system interacting with it through a classical electric-potential signal. Specifically, we show that direct control over two-level emitters is possible, thus allowing one to convert the excited state into a long-lived state and eliminating the need to involve additional excited or metastable states and external control fields on which other methods rely [1, 10]. Our results can be used for a robust, solid-state implementation of photon storage [21] and cascaded quantum systems in which one system drives the evolution of another system [22, 23]. These are the basic elements needed for distributed quantum networks and processors, and quantum state transfer.

The emergence of graphene as a tunable plasmonic material, in which plasmons can be literally switched on and off by applying external potentials [8], opens a natural way to control the quantum evolution of small systems through plasmon-mediated interactions, which are in turn modulated by external fields. Charge carriers in graphene, the so-called massless Dirac fermions, follow a linear dispersion relation that leads to several exciting properties. Among them, low-energy plasmons exist in the atomically thin carbon film when it is electrically charged, and their frequencies scale as $n^{1/4}$ with the doping electron density [24] n . Therefore, the plasmon frequencies can be controlled by changing n , which in turn is proportional to the magnitude of the applied electric field. This field can be supplied by biasing the graphene with respect to a nearby gate, and thus, the voltage applied through the gates directly modifies, in a predictable way, the plasmon frequencies.

Here, we show that the interaction between one or more quantum emitters and graphene plasmons strongly modifies the evolution of the system, which can be temporally controlled by switching on and off the plasmons through electrostatic gating. We first illustrate this concept by analyzing the interaction of a doped graphene nanodisc with a single quantum emitter (figure 1). The size of the disc is an important parameter that directly affects the plasmon frequency and the strength of the coupling to the emitter. Both these magnitudes decrease with increasing diameter.

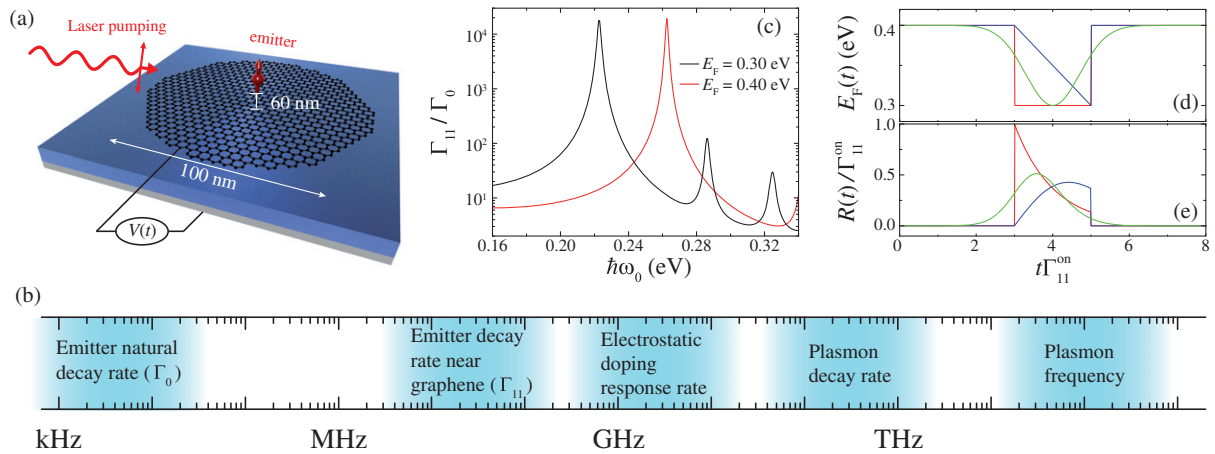


Figure 1. Temporal control over the quantum evolution of an optical emitter via interaction with a doped graphene nanostructure. (a) We consider a two-level optical emitter placed above a graphene nanodisc. The emitter is excited by a laser pulse. Electrical doping of the graphene through a bias potential V allows the nanodisc to support plasmons. The plasmon frequency is proportional to $\sqrt{|V|}$, and thus, it can be controlled over time by modulating $V(t)$. The coupling of the emitter to the plasmon and therefore the quantum evolution of the emitter state are both controlled by V . (b) Different time scales are involved in the evolution of the emitter–graphene system, represented here through the emitter natural decay rate Γ_0 , the enhanced decay rate Γ_{11} produced by interaction with the graphene plasmons and the plasmon decay rate and frequency typical of doped graphene. It is important to stress that the plasmon lifetime is short compared to the electric modulation rates of the doping potential, in the GHz range, which is in turn fast compared to the lifetime of the excited emitter. (c) The increase in emission rate Γ_{11}/Γ_0 is shown as a function of emission frequency for two different doping levels, quantified through the graphene Fermi energy E_F . The temporal profile of the emission rate $R(t)$ can be controlled by suitably modulating E_F over time as shown in (d) and (e) for $\hbar\omega_0 = 0.22$ eV.

Here, we choose a realistic nanodisc diameter of 100 nm, which is sufficiently large to ignore edge effects that are otherwise important in smaller discs below 20 nm in diameter [25]. The level of doping is characterized by the Fermi energy [26] $E_F = \hbar v_F \sqrt{\pi |n|}$, where $v_F \approx 10^6$ m s⁻¹ is the Fermi velocity. This determines the plasmon energy $\hbar\omega_p \propto \sqrt{E_F}$ and the plasmon decay rate [27] $\Gamma_p \propto 1/E_F$. The emitter is placed 60 nm above the center of the graphene nanodisc. This is a realistic geometry, considering recent advances in the control of the position and orientation of optical emitters [28–30]. One of the ways to facilitate such a control consists in depositing a passive dielectric layer above the graphene sheet, the thickness of which determines the separation from the emitters. Solid-state emitters based upon quantum dots or nitrogen vacancies embedded in nanodiamond crystals offer the additional possibility of coating them with silica [31], thus providing a controlled spacing distance depending on the thickness of the coating layer. We model the emitter as a two-level system with a characteristic transition energy $\hbar\omega_0$ and a natural decay rate Γ_0 . The different time scales that characterize the evolution

of the system are plotted in figure 1(b). We choose a value of $\Gamma_0 \sim 10^3\text{--}10^4 \text{ s}^{-1}$ typical of slowly emitting atoms such as erbium. When the emitter is placed close to the nanodisc, its decay rate is enhanced up to $\Gamma_{11} \sim 10^4 \Gamma_0$ due to resonant interaction with the graphene plasmons. These decay rates are well below the frequencies at which the doping level can be modulated with currently available electronics ($\sim\text{GHz}$), which in turn is much smaller than the plasmon frequency ω_p and the decay rate Γ_p . With this choice of parameters, we ensure that the emitter–plasmon interaction remains in the weak-coupling regime, instantaneously following any modulation of the doping level. Under such conditions, we can trace out the plasmonic degrees of freedom and therefore the dynamics of the quantum emitter is completely described by the reduced density matrix ρ , whose temporal evolution is given as [32]

$$\frac{d\rho}{dt} = \frac{i}{\hbar} [\rho, \mathcal{H}] + \frac{\Gamma_{11}}{2} [2\sigma\rho\sigma^\dagger - \sigma^\dagger\sigma\rho - \rho\sigma^\dagger\sigma], \quad (1)$$

where σ is the annihilation operator of the emitter excited state, and the Hamiltonian reduces to $\mathcal{H} = \hbar\omega_0\sigma^\dagger\sigma$. This is in contrast to the strong-coupling regime, which is, for instance, reached by decreasing the emitter–graphene separation and requires a full description of the density matrix including the emitter and the cavity modes, without tracing out the latter. This regime has recently been studied for graphene nanodiscs [20].

Incidentally, the electrostatic doping of the graphene nanodisc can influence the emitter spectrum by shifting the transition frequency through the Stark effect. This could be problematic in asymmetric systems unless the shifts are small compared with the plasmon line width. However, for symmetrical configurations such as the ones we consider here, all emitters experience the same frequency shift, and thus, this effect simply needs to be taken into account when considering the graphene plasmon frequency at which the emitters are on resonance.

Figure 1(c) shows the normalized decay rate Γ_{11}/Γ_0 as a function of emission energy $\hbar\omega_0$ for two different doping levels corresponding to Fermi energies of 0.3 and 0.4 eV, respectively. Then, choosing an emitter of transition energy ≈ 0.22 eV (the highest peak of the black curve), we can switch the normalized decay rate from $\Gamma_{11}^{\text{on}}/\Gamma_0 > 10^4$ down to $\Gamma_{11}^{\text{off}}/\Gamma_0 \sim 10$ just by shifting the graphene doping level from 0.3 to 0.4 eV. This clearly shows the feasibility of controlling the temporal evolution of the quantum emitter by modulating the doping level of the graphene nanodisc between on- and off-resonance conditions. We explore this possibility in more detail in figures 1(d) and (e) for three different doping modulation profiles: rectangular (red curve), triangular (blue curve) and Gaussian (green curve). The emitter is initially prepared in the excited state, and we study the plasmon generation rate $R = \langle \Gamma_{11}\sigma^\dagger\sigma \rangle$, normalized to Γ_{11}^{on} . This magnitude measures the number of plasmons generated per unit time, and it is calculated here neglecting decay channels other than plasmon generation. This assumption is well justified by the large values of $\Gamma_{11}^{\text{on/off}}/\Gamma_0$. As shown in figure 1(e), each different doping profile results in a totally different evolution of the quantum emitter, which reflects the complete temporal control achievable with the system under study. Actually, it is not difficult to obtain the analytical relation existing between R and the single-emitter decay rate. Assuming that the emitter is in its excited state at time $t = t_0$, this relation reduces to

$$\Gamma_{11}(t) = \frac{R(t)}{1 - \int_{t_0}^t dt' R(t')}.$$

With the only constraint that $\Gamma_{11}(t) \leq \Gamma_{11}^{\text{on}}$, the desired profile $R(t)$ can be achieved with the temporal evolution of $\Gamma_{11}(t)$ prescribed by this equation, which in turn is obtained by directly

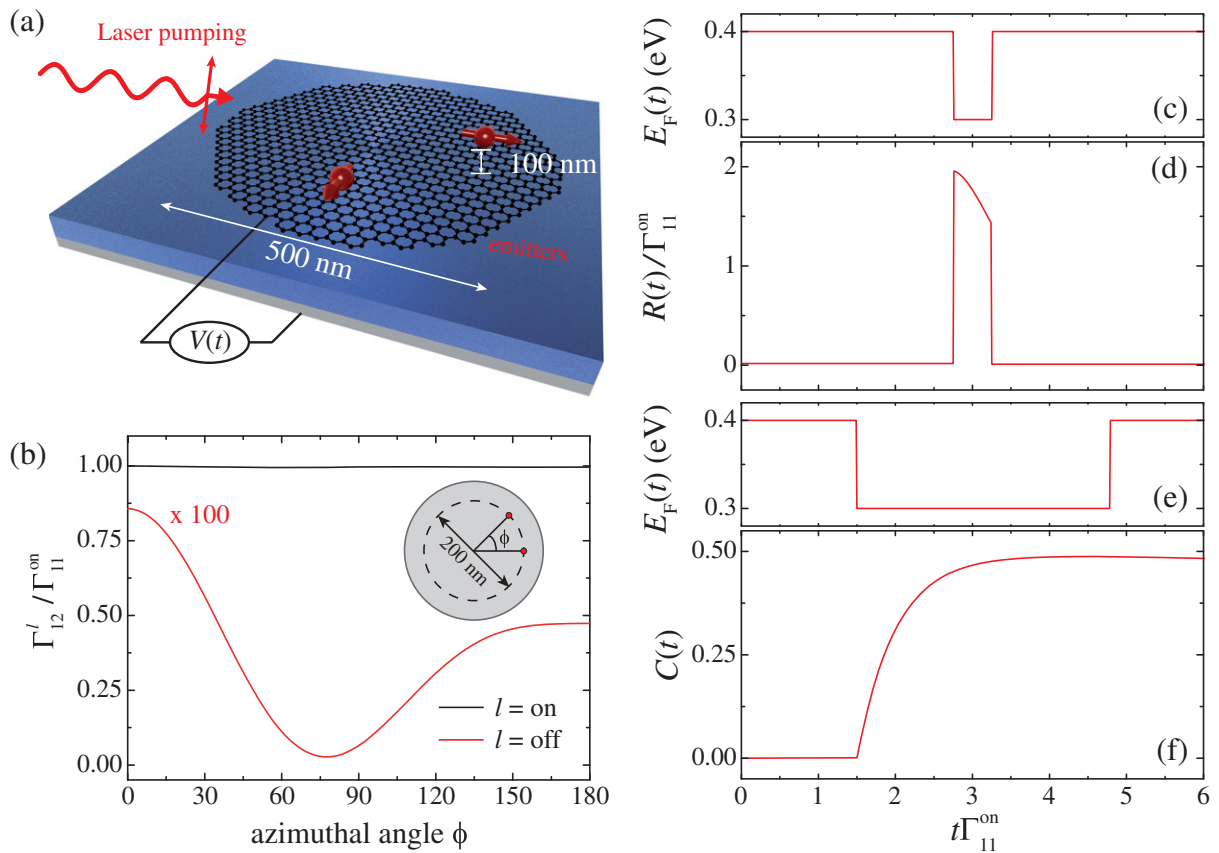


Figure 2. Temporal control over the interaction between quantum dots mediated by graphene. (a) Two emitters are excited and their decay and mutual interaction is modulated electrically through the plasmons of a neighboring graphene disc. (b) Interaction rate Γ_{12} as a function of the azimuthal angle between the positions of the dots (see the inset) when plasmons of 0.108 eV energy (tuned to the energy of the dots) are switched on ($E_F = 0.3$ eV) and off ($E_F = 0.4$ eV), and the emitter dipoles are along radial directions. The interaction rate is normalized to the on-resonance single-emitter decay rate Γ_{11}^{on} . The imposed temporal evolution of the doping (c) is used to control the emission rate (d) with the two emitters initially prepared in their excited states. When only one of the emitters is initially excited, the degree of entanglement for the doping profile of (e) is quantified through the Wooters concurrence (f).

modulating the doping voltage, and therefore E_F , over time by using the Lorentzian dependence of Γ_{11} on E_F discussed in detail in appendix B.

When a second quantum emitter is placed close to the graphene, the interaction between the two emitters can also be controlled over time. The interaction between two emitters in extended graphene and in ribbons has recently been shown to be strongly enhanced or suppressed by the plasmons [33]. We investigate this possibility by studying the system depicted in figure 2(a), where two identical emitters are placed 100 nm above a graphene nanodisc of 500 nm diameter. The emitters are separated by a distance of $100\sqrt{2}$ nm and oriented along orthogonal radial directions, so that they can be independently excited by light plane waves linearly polarized

along orthogonal directions. Their temporal evolution is determined by the generalization of (1),

$$\frac{d\rho}{dt} = \frac{i}{\hbar} [\rho, \mathcal{H}] + \sum_{i,j=1}^2 \frac{\Gamma_{ij}}{2} \left[2\sigma_i \rho \sigma_j^\dagger - \sigma_i^\dagger \sigma_j \rho - \rho \sigma_i^\dagger \sigma_j \right], \quad (2)$$

where $\mathcal{H} = \hbar\omega_0 \sum_{i=1}^2 \sigma_i^\dagger \sigma_i$ and $\Gamma_{12} = \Gamma_{21}$ is the interaction rate. This magnitude is plotted in figure 2(b) as a function of the azimuthal angle between the emitters, normalized to the on-resonance single-emitter decay rate Γ_{11}^{on} . When the doping level of the graphene nanodisc matches the on-resonance value, Γ_{12} remains nearly equal to Γ_{11}^{on} for all angles. In contrast, the normalized interaction rate $\Gamma_{12}/\Gamma_{11}^{\text{on}}$ drops below 0.01 when the doping is tuned to off-resonance conditions. Therefore, it is possible to switch on and off the interaction between the emitters. Figure 2(d) quantifies this possibility through the temporal evolution of the plasmon generation rate $R = \langle \sum_{i,j=1}^2 \Gamma_{ij} \sigma_i^\dagger \sigma_j \rangle$ associated with the doping profile shown in figure 2(c). The two emitters are assumed to be initially prepared in the excited state. Without interaction, they decay rather slowly and independently, resulting in a negligible value of R . This situation changes dramatically when the doping level is switched to the on-resonance condition, so that the emitters interact strongly and decay faster, causing a sudden jump in the plasmon generation rate.

The high degree of control displayed by this system can be exploited to temporally modulate different properties of the quantum emitters, such as their degree of entanglement. In figure 2(f) we plot the temporal evolution of the Wootters concurrence [34] (see appendix D) associated with the doping profile of figure 2(e) when only one of the emitters is initially excited. The concurrence directly measures the degree of entanglement (1 for a maximally entangled state). Our system is capable of reaching a value of C close to 0.5, which is understandable because a single excited emitter can be rewritten as a mixture of a symmetric (superradiant) state and an anti-symmetric (subradiant) state, but the subradiant state lives for a very long time, such that there is a 50% chance of creating a long-lived entangled state. A larger degree of entanglement can be achieved by various means, such as utilizing quantum emitters with more than two levels, heralded schemes based on photon detection or coherent dipole–dipole interactions between the emitters.

A similar scheme allows the on-demand modulation of the emission in systems consisting of many emitters, in which superradiance [35, 36] can be produced and controlled electrostatically. Such a possibility is discussed in more detail in appendix C.

In summary, we demonstrate here that electrical modulation of the plasmon frequency in graphene provides an ingenious solution to achieve temporal control of the evolution of quantum emitters placed in the vicinity of a graphene nanostructure. This leads to a new paradigm in quantum information processing technologies and serves as a platform on which to test quantum phenomena controlled by means of externally applied, classical electrostatic potentials.

Acknowledgments

This work was supported by the Spanish Ministerio de Educación (MAT2010-14885 and Consolider NanoLight.es) and the European Commission (FP7-ICT-2009-4-248909-LIMA and FP7-ICT-2009-4-248855-N4E). DEC acknowledges support from Fundacio Privada Cellex Barcelona. AM acknowledges financial support through FPU from the Spanish Ministerio de Educación.

Appendix A. Simulation of the optical response of graphene

We calculate the emission rates Γ_{11} and Γ_{12} by following methods reported elsewhere [27, 37, 38]. The optical response of graphene is obtained by solving Maxwell's equations in the presence of an emitter dipole [37]. The graphene is represented by a thin film of dielectric function $\epsilon = 1 + 4\pi i\sigma/\omega t$, where ω is the frequency, $t \rightarrow 0$ is the film thickness and $\sigma(\omega)$ is the optical conductivity of the carbon layer, described within the local random-phase approximation model for finite temperature $T = 300$ K and mobility $10\,000 \text{ cm}^2 \text{ V}^{-1} \text{ s}^{-1}$. The rate Γ_{11} is then obtained from the imaginary part of the electric field \mathbf{E}^{ind} induced on itself by a dipole \mathbf{d} placed at the position of the emitter [37]: $\Gamma_{11}/\Gamma_0 = 1 + (2/\hbar)\text{Im}\{\mathbf{d}^* \cdot \mathbf{E}^{\text{ind}}\}$, where $\Gamma_0 = 4\omega^3|\mathbf{d}|^2/3\hbar c^3$ is the natural emission rate far from the graphene. Likewise, Γ_{12} is obtained using the expression [38]

$$\Gamma_{12} = \frac{2}{\hbar}\text{Im}\{\mathbf{d}_1^* \cdot \mathbf{E}_{12}\}, \quad (\text{A.1})$$

where \mathbf{d}_1 is the dipole of emitter 1, and \mathbf{E}_{12} is the field created by the dipole of emitter 2 at the position of emitter 1, including both the direct dipolar field and the field due to the excitation of the graphene plasmon.

Appendix B. Dependence of Γ_{11} on the Fermi energy

In order to design an appropriate doping profile and obtain an on-demand temporal evolution of the quantum state of the emitter, it is important to analyze the dependence of the single-emitter decay rate Γ_{11} on the Fermi energy of the graphene nanodisc. Figure B.1 shows this dependence. More precisely, we plot Γ_{11}/Γ_0 as a function of E_F for the case of a nanodisc of 100 nm diameter with the emitter placed 60 nm above its center. This corresponds to the system depicted in figure 1(a) of the main text, with the same photon energy $\hbar\omega_0 = 0.22$ eV. The black points in figure B.1 correspond to rigorous numerical simulations [27], while the red curve represents the following Lorentzian fitting:

$$\frac{\Gamma_{11}}{\Gamma_0}(E_F) = \left(\frac{\Gamma_{11}}{\Gamma_0}\right)_0 + \frac{(\Gamma_{11}/\Gamma_0)_{\text{max}}\tau^2/4}{(E_F - E_{F0}) + \tau^2/4}, \quad (\text{B.1})$$

with $(\Gamma_{11}/\Gamma_0)_0 = 1.96$, $(\Gamma_{11}/\Gamma_0)_{\text{max}} = 18\,635.6$, $E_{F0} = 0.3$ eV and $\tau = 5.21 \times 10^{-3}$ eV.

Appendix C. Controlled superradiance of N emitters

A scheme similar to the one discussed in figure 2 can be used to control the evolution of an ensemble of emitters coupled to a graphene nanodisc. In particular, these emitters can be brought in a controlled manner to a superradiance regime [35, 36, 39–41] in which they are collectively coupled. We illustrate this possibility by studying the system depicted in figure C.1(a). We consider a nanodisc of 500 nm diameter, with N emitters periodically arranged along a co-axial circumference of 200 nm diameter, placed 100 nm above the disc. The emitters are polarized perpendicularly to the graphene nanodisc and we assume a transition frequency $\hbar\omega_0 = 0.108$ eV, compatible with an on-resonance (off-resonance) Fermi energy of $E_F^{\text{on}} = 0.3$ eV ($E_F^{\text{off}} = 0.4$ eV). The interaction rate between pairs of emitters Γ_{12} is plotted in figure C.1(b) as a function of their relative azimuthal angle along the noted circumference, normalized to the on-resonance single-emitter decay rate Γ_{11}^{on} .

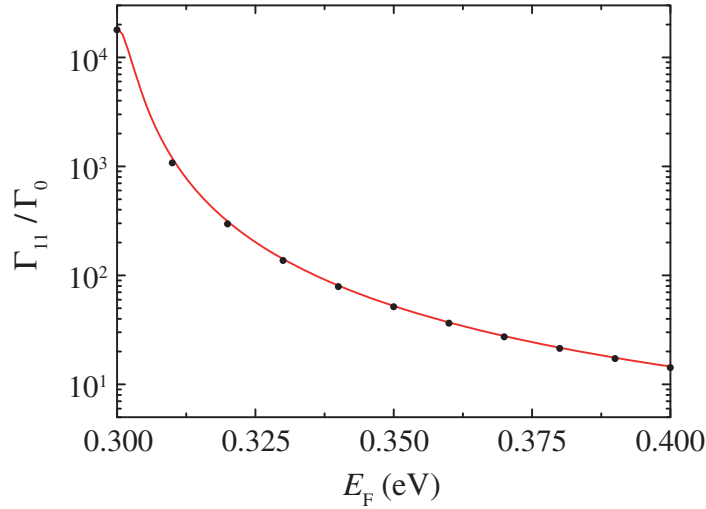


Figure B.1. Dependence of the single-emitter decay rate Γ_{11} on the Fermi energy. We consider the system depicted in figure 1(a) of the main text: the nanodisc has a diameter of 100 nm, the quantum emitter is placed at a distance of 60 nm above the center of the graphene disc, and we set the photon energy to $\hbar\omega_0 = 0.22$ eV. Black points are a rigorous numerical simulation, while the red curve represents the Lorentzian fitting of (B.1).

The temporal dynamics of the system is given by a generalized version of (2), with the sums extended over the N emitters. This is a straightforward task for small N , but it becomes unaffordable above $N \sim 10$ because the resulting Hilbert space grows exponentially with N . However, under perfectly symmetric coupling conditions ($\Gamma_{12} = \Gamma_{11}$ for all pairs of emitters), as is the case in our system when $E_F = E_F^{\text{on}}$, the temporal evolution is simplified because only symmetrical combinations of the single-emitter states are involved in the dynamics of the system [36]. These symmetrical states are characterized by a single quantum number M , which can take values in the interval $-N/2, \dots, N/2$, where $M + N/2$ is the number of emitters that are in the excited state. Using this notation, it has been proved [36] that the generalization of (2) reduces to

$$\frac{1}{\Gamma_{11}} \frac{d\rho_M}{dt} = - \left(\frac{N}{2} + M \right) \left(\frac{N}{2} - M + 1 \right) \rho_M + \left(\frac{N}{2} + M + 1 \right) \left(\frac{N}{2} - M \right) \rho_{M+1},$$

which can be quickly solved for a large number of emitters. Furthermore, the small values of Γ_{12}^{off} allow us to safely assume a system of independent emitters under off-resonance doping conditions. At this point, it is important to remark that we have not explicitly considered the coherent coupling existing between the emitters. In principle, this coupling produces a shift of the transition energies that can destroy the superradiance regime. However, for systems like ours in which all emitters are placed in symmetrically equivalent positions, the shift is the same for all, so we absorb it into the final transition energy $\hbar\omega_0$.

As a particular example to illustrate the concepts discussed here, we study the dynamics of $N = 10$ emitters controlled using the temporal doping profile shown in figure C.1(c). We assume that all emitters are initially prepared in the excited state, and we normalize all rates and the time using Γ_{11}^{on} . Figure C.1(d) shows the plasmon generation rate R . Initially, the emitters

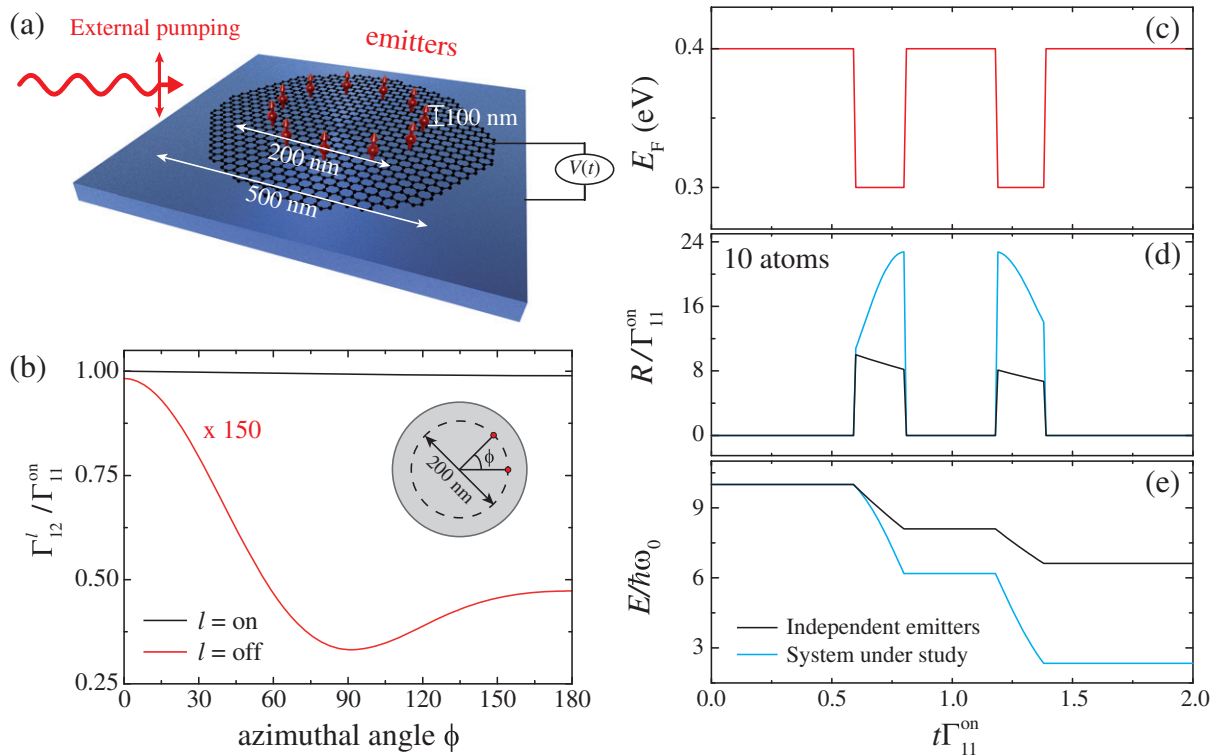


Figure C.1. Control of the superradiance emission from an ensemble of emitters coupled to a graphene nanodisc. (a) N two-level quantum emitters are periodically arranged along a circumference of 200 nm diameter placed 100 nm above a doped graphene nanodisc of 500 nm diameter. The combined system possesses N -fold rotation symmetry with the emitter dipoles oriented perpendicular to the disc. The system is pumped with an external laser that brings all emitters to the excited state at time $t = 0$. (b) Interaction rate Γ_{12} as a function of the azimuthal angle between the positions of the emitters (see the inset) when plasmons of 0.108 eV energy (tuned to the energy of the emitters) are switched on ($E_F^{\text{on}} = 0.3$ eV) and off ($E_F^{\text{off}} = 0.4$ eV). The interaction rate is normalized to the on-resonance single-emitter decay rate Γ_{11}^{on} . (c) Illustrative doping level of the graphene nanostructure as a function of time (normalized to $1/\Gamma_{11}^{\text{on}}$). (d) Plasmon generation rate as a function of time for $N = 10$ emitters subject to the time-dependent doping of (c). The black curve stands for the case of independent emitters (i.e. imposing $\Gamma_{12} = 0$), while the blue one corresponds to the fully interacting system. The plasmon generation rate is strongly enhanced by the collective superradiance effect produced by the coupling between the emitters. (e) The amount of energy released by the emitters as a function of time under the conditions of (d). Superradiance produces a considerably faster energy release.

decay very slowly and independently, resulting in a negligible value of R . The situation changes dramatically when the doping is switched to the on-resonance level, at which the emitters decay faster, producing a sudden jump in the plasmon generation rate. In the independent emitters limit (black curve), the maximum rate is $R/\Gamma_{ii}^{\text{on}} = N$. In contrast, under resonant coupling (blue curves), $R/\Gamma_{ii}^{\text{on}}$ goes beyond N for $N > 2$ (superradiance regime). A high emission rate

is repeatedly recovered when the doping is switched off and on at later times, thus revealing a high degree of control over the system dynamics.

Figure C.1(e) shows the amount of energy stored in the emitters as a function of time. As expected, this magnitude remains close to $N\hbar\omega_0$ until a resonant doping is switched on. When this happens, the emitters release their excitation energy during the time in which $E_F = E_F^{\text{on}}$.

Appendix D. Calculation of the Wootters concurrence

The degree of entanglement existing in a two-qubit system can be quantified using the definition of the concurrence C proposed by Wootters [34]

$$C = \max \left\{ 0, \sqrt{\lambda_1} - \sqrt{\lambda_2} - \sqrt{\lambda_3} - \sqrt{\lambda_4} \right\}, \quad (\text{D.1})$$

where λ_i are the eigenvalues of the matrix $\rho(\sigma_y \otimes \sigma_y)\rho^*(\sigma_y \otimes \sigma_y)$, ordered from large to small values. Here, ρ is the density matrix, σ_y is the Pauli matrix and the asterisk stands for the complex conjugate. In the particular case considered in figure 2(c), we assume that one of the emitters is excited while the other is in the ground state (e.g. $|\psi\rangle = |eg\rangle$). In such a situation, the concurrence reduces to

$$C = \sqrt{[\rho_{++} - \rho_{--}]^2 + 4[\Im\{\rho_{+-}\}]^2}, \quad (\text{D.2})$$

where $\rho_{ss'} = \langle s|\rho|s'\rangle$ with $s, s' \in \{+, -\}$, and $|\pm\rangle = (1/\sqrt{2})[|eg\rangle \pm |ge\rangle]$.

References

- [1] Cirac J I, Zoller P, Kimble H J and Mabuchi H 1997 Quantum state transfer and entanglement distribution among distant nodes in a quantum network *Phys. Rev. Lett.* **78** 3221–4
- [2] Amini J M, Uys H, Wesenberg J H, Seidelin S, Britton J, Bollinger J J, Leibfried D, Ospelkaus C, VanDevender A P and Wineland D J 2010 Toward scalable ion traps for quantum information processing *New J. Phys.* **12** 033031
- [3] Ritter S, Nolleke C, Hahn C, Reiserer A, Neuzner A, Uphoff M M, Mucke Figueroa E, Bochmann J and Rempe G 2012 An elementary quantum network of single atoms in optical cavities *Nature* **484** 195–200
- [4] Ladd T D, Jelezko F, Laflamme R, Nakamura Y, Monroe C and O'Brien J L 2010 Quantum computers *Nature* **464** 45–53
- [5] Togan E *et al* 2010 Quantum entanglement between an optical photon and a solid-state spin qubit *Nature* **466** 730–4
- [6] Li Z Q, Henriksen E A, Jian Z, Hao Z, Martin M C, Kim P, Stormer H L and Basov D N 2008 Dirac charge dynamics in graphene by infrared spectroscopy *Nature Phys.* **4** 532–5
- [7] Chen C F *et al* 2011 Controlling inelastic light scattering quantum pathways in graphene *Nature* **471** 617–20
- [8] Chen J *et al* 2012 Optical nano-imaging of gate-tunable graphene plasmons *Nature* **487** 77–81
Fei Z *et al* 2012 Gate-tuning of graphene plasmons revealed by infrared nano-imaging *Nature* **487** 82–5
- [9] Yamamoto N, Ohtani S and García de Abajo F J 2011 Gap and Mie plasmons in individual silver nanospheres near a silver surface *Nano Lett.* **11** 91–5
- [10] Duan L M and Monroe C 2008 Robust probabilistic quantum information processing with atoms, photons and atomic ensembles *Advances in Atomic, Molecular and Optical Physics* vol 55, ed E Arimondo, P R Berman and C C Lin (New York: Academic) pp 419–63

- [11] Kimble H J 2008 The quantum internet *Nature* **453** 1023–30
- [12] Dowling P J 2008 Quantum optical metrology—the lowdown on high-noon states *Contemp. Phys.* **49** 125–43
- [13] Mandel L 1986 Non-classical states of the electromagnetic field *Phys. Scr.* **12** 34–42
- [14] Ourjoumtsev A, Tualle-Brouiri R, Laurat J and Grangier P 2006 Generating optical Schrödinger kittens for quantum information processing *Science* **312** 83–6
- [15] Afek I, Ambar O and Silberberg Y 2010 High-noon states by mixing quantum and classical light *Science* **328** 879–81
- [16] Nielsen M A and Chuang I L 2004 *Quantum Computation and Quantum Information* 1st edn (Cambridge Series on Information and the Natural Sciences) (Cambridge: Cambridge University Press)
- [17] van Enk S J, Cirac J I and Zoller P 1997 Ideal quantum communication over noisy channels: a quantum optical implementation *Phys. Rev. Lett.* **78** 4293–6
- [18] Chang D E, Sorensen A S, Demler E A and Lukin M D 2007 A single-photon transistor using nanoscale surface plasmons *Nature Phys.* **3** 807–12
- [19] Gonzalez-Tudela A, Martin-Cano D, Moreno E, Martin-Moreno L, Tejedor C and Garcia-Vidal F J 2011 Entanglement of two qubits mediated by one-dimensional plasmonic waveguides *Phys. Rev. Lett.* **106** 020501
- [20] Manjavacas A, Nordlander P and García de Abajo F J 2012 Plasmon blockade in nanostructured graphene *ACS Nano* **6** 1724–31
- [21] Gorshkov A V, André A, Fleischhauer M, Sørensen A S and Lukin M D 2007 Universal approach to optimal photon storage in atomic media *Phys. Rev. Lett.* **98** 123601
- [22] Gardiner C W 1993 Driving a quantum system with the output field from another driven quantum system *Phys. Rev. Lett.* **70** 2269–72
- [23] Carmichael H J 1993 Quantum trajectory theory for cascaded open systems *Phys. Rev. Lett.* **70** 2273–6
- [24] Jablan M, Buljan H and Soljačić M 2009 Plasmonics in graphene at infrared frequencies *Phys. Rev. B* **80** 245435
- [25] Thongrattanasiri S, Manjavacas A and García de Abajo F J 2012 Quantum finite-size effects in graphene plasmons *ACS Nano* **6** 1766–75
- [26] Castro Neto A H, Guinea F, Peres N M R, Novoselov K S and Geim A K 2009 The electronic properties of graphene *Rev. Mod. Phys.* **81** 109–62
- [27] Koppens F H L, Chang D E and García de Abajo F J 2011 Graphene plasmonics: a platform for strong light–matter interactions *Nano Lett.* **11** 3370–7
- [28] Curto A G, Volpe G, Taminiu T H, Kreuzer M P, Quidant R and van Hulst N F 2010 Unidirectional emission of a quantum dot coupled to a nanoantenna *Science* **329** 930–3
- [29] Andreas Lieb M, Zavislan J M and Novotny L 2004 Single-molecule orientations determined by direct emission pattern imaging *J. Opt. Soc. Am. B* **21** 1210–5
- [30] Kukura P, Ewers H, Muller C, Renn A, Helenius A and Sandoghdar V 2009 High-speed nanoscopic tracking of the position and orientation of a single virus *Nature Methods* **6** 923–7
- [31] Ung T, Liz-Marzán L M and Mulvaney P 2001 Optical properties of thin films of Au@SiO₂ particles *J. Phys. Chem. B* **105** 3441–52
- [32] Ficek Z and Tanas R 2002 Entangled states and collective nonclassical effects in two-atom systems *Phys. Rep.* **372** 369–443
- [33] Huidobro P A, Nikitin A Y, González-Ballester C, Martín-Moreno L and García-Vidal F J 2012 Superradiance mediated by graphene surface plasmons *Phys. Rev. B* **85** 155438
- [34] Wootters W K 1998 Entanglement of formation of an arbitrary state of two qubits *Phys. Rev. Lett.* **80** 2245–8
- [35] Dicke R H 1954 Coherence in spontaneous radiation processes *Phys. Rev.* **93** 99–110
- [36] Gross M and Haroche S 1982 Superradiance: an essay on the theory of collective spontaneous emission *Phys. Rep.* **93** 301–96
- [37] Novotny L and Hecht B 2006 *Principles of Nano-Optics* (New York: Cambridge University Press)
- [38] Dzsotjan D, Sorensen A S and Fleischhauer M 2010 Quantum emitters coupled to surface plasmons of a nanowire: a Green’s function approach *Phys. Rev. B* **82** 075427

- [39] Skribanowitz N, Herman I P, MacGillivray J C and Feld M S 1973 Observation of Dicke superradiance in optically pumped HF gas *Phys. Rev. Lett.* **30** 309–12
- [40] Gross M, Fabre C, Pillet P and Haroche S 1976 Observation of near-infrared Dicke superradiance on cascading transitions in atomic sodium *Phys. Rev. Lett.* **36** 1035–8
- [41] Inouye S, Chikkatur A P, Stamper-Kurn D M, Stenger J, Pritchard D E and Ketterle W 1999 Superradiant Rayleigh scattering from a Bose–Einstein condensate *Science* **285** 571–4